Identification and functional characterization of a novel heterozygous splice-site mutation in the calpain 3 gene causes rare autosomal dominant limb-girdle muscular dystrophy

BIN MAO[1*], JIE YANG[1*], XIAODONG ZHAO[1], XUELING JIA[1], XIN SHI[1], LIHUI ZHAO[1], SANTASREE BANERJEE[2], LILI ZHANG[1] and XIAOLING MA[1]

[1]The Reproductive Medicine Centre, The First Hospital of Lanzhou University, Lanzhou, Gansu 730000; [2]Department of Genetics, College of Basic Medical Sciences, Jilin University, Changchun, Jilin 130021, P.R. China

Received August 30, 2022; Accepted November 3, 2023

DOI: 10.3892/etm.2024.12385

Abstract. Limb-girdle muscular dystrophies are a group of extremely heterogenous neuromuscular disorders that manifest with gradual and progressive weakness of both proximal and distal muscles. Autosomal dominant limb-girdle muscular dystrophy (LGMDD4) or calpainopathy is a very rare form of myopathy characterized by weakness and atrophy of both proximal and distal muscles with a variable age of onset. LGMDD4 is caused by germline heterozygous mutations of the calpain 3 (*CAPN3)* gene. Patients with LGMDD4 often show extreme phenotypic heterogeneity; however, most patients present with gait difficulties, increased levels of serum creatine kinase, myalgia and back pain. In the present study, a 16-year-old male patient, clinically diagnosed with LGMDD4, was investigated. The proband had been suffering from weakness and atrophy of both of their proximal and distal muscles, and had difficulty walking and standing independently. The serum creatine kinase levels (4,754 IU/l; normal, 35-232 IU/l) of the patient were markedly elevated. The younger sister and mother of the proband were also clinically diagnosed with LGMDD4, while the father was phenotypically normal. Whole exome sequencing identified a heterozygous novel splice-site (c.2440-1G>A) mutation in intron 23 of the *CAPN3* gene in the proband. Sanger sequencing confirmed that this mutation was also present in both the younger sister and mother of the proband, but the father was not a carrier of this mutation. This splice-site (c.2440-1G>A) mutation causes aberrant splicing of CAPN3 mRNA, leading to the skipping of the last exon (exon 24) of CAPN3 mRNA and resulting in the removal of eight amino acids from the C-terminal of domain IV of the CAPN3 protein. Hence, this splice site mutation causes the formation of a truncated CAPN3 protein (p.Trp814*) of 813 amino acids instead of the wild-type CAPN3 protein that consists of 821 amino acids. This mutation causes partial loss of domain IV (PEF domain) in the CAPN3 protein, which is involved in calcium binding and homodimerization; therefore, this is a loss-of-function mutation. Relative expression of the mutated CAPN3 mRNA was reduced in comparison with the wild-type CAPN3 mRNA in the proband, and their younger sister and mother. This mutation was also not present in 100 normal healthy control individuals of the same ethnicity. The present study reported the first case of *CAPN3* gene-associated LGMDD4 in the Chinese population.

Correspondence to: Dr Lili Zhang or Dr Xiaoling Ma, The Reproductive Medicine Centre, The First Hospital of Lanzhou University, 1 Donggangxi Road, Chengguan, Lanzhou, Gansu 730000, P.R. China
E-mail: 13893486294@139.com
E-mail: maxl2005@163.com

*Contributed equally

Key words: limb-girdle muscular dystrophy, *CAPN3* gene, novel mutation, whole exome sequencing, splice-site mutation, autosomal dominant

Introduction

Limb-girdle muscular dystrophies (LGMDs) are a major group of muscular dystrophies with extreme genotypic and phenotypic heterogeneity (1). LGMDs were first classified as autosomal dominant (LGMDD4, MIM#618129) or autosomal recessive (LGMD2A, MIM#253600) by the European Neuromuscular Centre in 1995 (2). The incidence of LGMD is ~1 in 100,000 live births worldwide with a variable age of onset (3). LGMD2A is the most common type of LGMD and accounts for ~30% of all cases; however, cases of LGMDD4 or calpainopathy are very rarely reported (4,5). Patients with LGMDD4 usually manifest with gradual, progressive weakness and atrophy of proximal muscles more than distal muscles, leading to difficulties in walking and running, a waddling gait, scapular winging and respiratory failure at the advanced stages of the disease (6). Furthermore, thigh muscles, pelvic girdle muscles, periscapular muscles and biceps are the most affected areas, with effects on the facial muscles rare (6,7). Patients with LGMDD4 are generally identified by elevated levels of serum creatine kinase, dystrophic changes in muscle pathology, and low or reduced expression

of calpain 3 (*CAPN3*) (7). A germline heterozygous mutation in the *CAPN3* gene causes autosomal dominant calpainopathy (LGMDD4) (8-10). Among the reported variants of the *CAPN3* gene, the most common are missense mutations (70%) with 30% accounting for loss-of-function variants, i.e., frameshift, nonsense and splice site variants (11).

The *CAPN3* gene is located on chromosome 15 and encodes the CAPN3 protein (9,10). CAPN3 is a member of the calpain superfamily and is a calcium-dependent non-lysosomal cysteine protease (11). CAPN3 is broadly distributed in myocytes and sarcomeres, and has a significant role in maintaining calcium homeostasis, regulating muscle contraction and stabilizing the motility of sarcomere cells (12-14). CAPN3 also plays a key role in the regulation of cell differentiation, apoptosis and the cell cycle.

At present, very few LGMDD4 cases have been reported worldwide (10,15-17). Vissing *et al* (10) reported a novel heterozygous 21-bp in-frame deletion (c.643_663del21, p.Ser215_Gly221del) in the *CAPN3* gene in European families with LGMDD4. Martinez-Thompson *et al* (15) also reported LGMDD4 due to the same heterozygous 21-bp in-frame deletion (c.643_663del21, p.Ser215_Gly221del) in the *CAPN3* gene in American families. This deletion is located in domain I (NS domain) of CAPN3 protein and results in a reduction in the rigidity of domain I and decreased inter-domain interactions with domain III, facilitating CAPN3 inactivation. Furthermore, Cerino *et al* (16) reported a novel *CAPN3* variant (c.1333G>A; p.Gly445Arg) that caused LGMDD4 in patients from four unrelated families. This variant is located in domain III (C2-like domain) of CAPN3 protein and causes impairment of the catalytic activity of mutated CAPN3 protein. This variant interacts with domain IV (PEF domain), which has a major role in calcium-binding and homodimerization of CAPN3. Finally, González-Mera *et al* (17) reported five heterozygous *CAPN3* missense variants (c.700G>A, p.Gly234Arg; c.1327T>C, p.Ser443Pro; c.1333G>A, p.Gly445Arg; c.1661A>C, p.Tyr554Ser and c.1706T>C, p.Phe569Ser) that caused LGMDD4 in seven unrelated families. The first variant (p.Gly234Arg) is located at domain I (NS domain) and induces the loss of the nuclear localization signal. However, all other variants (p.Ser443Pro, p.Gly445Arg, p.Tyr554Ser and p.Phe569Ser) are located in domain III and cause impairment of CAPN3 activation by calmodulin. It is critical that more cases of LGMDD4 are reported on in the future to gain an improved understanding of the disease mechanism and inheritance patterns (18,19).

In the present study, a 16-year-old male patient with gradual and progressive weakness, and atrophy of the muscles in both legs was investigated. The younger sister and mother of the proband exhibited the same phenotypes as the proband. Whole exome sequencing was performed to identify the disease-causing variant, followed by functional characterization of this disease-causing variant to demonstrate its pathogenicity.

Materials and methods

Subjects. A 16-year-old male patient clinically diagnosed with LGMDD4 from a nonconsanguineous Han Chinese family was investigated (Fig. 1A). The mother and younger sister of the proband were also clinically diagnosed with LGMDD4 while the father was phenotypically normal.

Muscle biopsy. A muscle biopsy was performed for the proband. Frozen sections of skeletal muscle were evaluated at The Reproductive Medicine Centre, The First Hospital of Lanzhou University (Lanzhou, China).

Fresh frozen sections of skeletal muscle. Excess moisture was first removed from the skeletal tissue sample simply by blotting thoroughly with a paper towel. Optimal cutting temperature compound was placed in the bottom of a shallow cryomold to provide a foundation for the section of muscle. The skeletal muscle section was carefully placed into the mold. Isopentane (2-methylbutane), which has a high thermal conductivity, does not form a vapor halo. Therefore, isopentane chilled with liquid nitrogen freezes muscle tissues more effectively and evenly than putting the tissues directly into liquid nitrogen. Therefore, prechilled isopentane was then chilled and maintained at -140˚C in a flask by adding liquid nitrogen. Then, the skeletal muscle section was kept in isopentane for 10-20 sec. Fresh frozen sections of skeletal muscle were stored at -80˚C. Then, cryo-sectioning of the frozen sections of skeletal muscles was performed and 10-μm sections were produced (20). These slides were processed further for staining.

Hematoxylin and eosin (H&E) staining. Slides were incubated at room temperature with hematoxylin solution for 10 min and washed with distilled water. Next, the slides were stained with eosin solution for 5 min at room temperature, followed by treatment with ethanol [70% ethanol for 30 sec, 90% ethanol for 30 sec and absolute (100%) ethanol for 1 min] at room temperature and finally xylene for 3 min at room temperature (21). Then, the slides were air-dried, mounted with xylene and stored at room temperature. Digital microscopy (variation of a traditional optical/light microscope; total magnification, x200) was used to capture the H&E-stained images.

Nicotinamide adenine dinucleotide dehydrogenase (NADH) staining. Firstly, TRIS buffer (0.05 M, pH 7.6), NADH solution, Nitro blue tetrazolium (NBT) solution and acetone de-staining solutions (30, 60 and 90%) were prepared. The NADH solution was gently thawed and 5 ml NBT solution was added to it. The slides were incubated in this solution for 30 min at 37˚C and washed three times with deionized water. The slides were washed again with acetone de-staining solutions first in increasing and then in decreasing concentrations. Finally, the slides were rinsed three times with deionized water and mounted with glycerol and phenol (22). A light microscope (total magnification, x200) was used to capture the images.

Immunohistochemistry analysis. The frozen skeletal tissue block was transferred to a cryotome cryostat at -20˚C prior to sectioning and the temperature of the frozen skeletal muscle tissue block was allowed to equilibrate to the temperature of the cryotome cryostat. Sections of the frozen skeletal muscle tissue block of the desired thickness (3, 5 and 8 μm) were prepared. Then, the skeletal muscle tissue sections were placed onto glass slides suitable for immunohistochemistry.

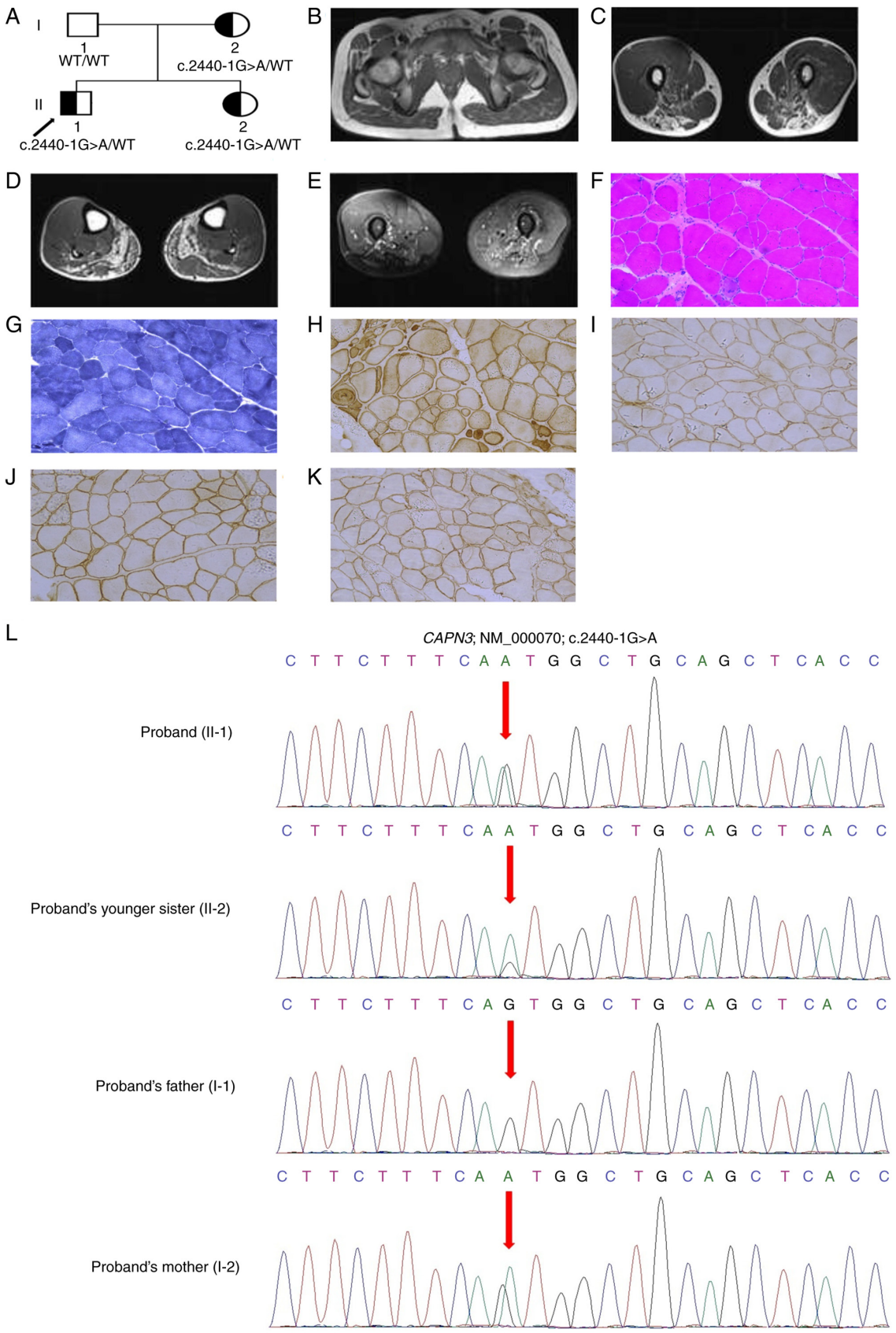

Figure 1. (A) Pedigree of the family. The squares indicate male patients and the circles indicate female patients. The half-filled symbols indicate affected patients (including the proband) and the empty symbols indicate unaffected healthy individuals. The arrow points to the proband. (B) Muscle magnetic resonance imaging of the proband showed severe involvement of adductor magnus, thigh muscles (biceps femoris, semimembranosus and semitendinosus) and calf muscles (gastrocnemius and soleus). (C) Hypertrophy of gracilis was identified. (D) Normal appearance of the rectus femoris, quadriceps femoris and sartorius of thigh muscles, was identified. (E) Normal appearance of tibialis anterior, tibialis posterior and extensor digitorum longus of calf muscles was found. (F-K) Muscle biopsy of the proband, (F) H&E, (G) NADH, (H) caveolin-3, (I) Dys, (J) α-sarcoglycan and (K) β-sarcoglycan staining. Total magnification, x200. (L) Partial DNA sequences in the *CAPN3* gene [NM_000070], as determined by Sanger sequencing of the proband, their younger sister and parents. Arrows point to the mutation. *CAPN3*, calpain 3; H&E, hematoxylin and eosin; NADH, nicotinamide adenine dinucleotide dehydrogenase; Dys, dystrophin.

Next, these sections were dipped in distilled water and treated with 5% hydrogen peroxidase for endogenous peroxidase blocking and incubated for 30 min at room temperature. Then, these sections were incubated with BondTM Primary Antibody Diluent 0.5L (cat. no. AR9352; Leica Microsystems, Inc.) at room temperature for 30 min for non-specific background blocking. Immunohistochemical analysis of skeletal muscle samples was performed with four primary antibodies (dystrophin, α-sarcoglycan, β-sarcoglycan and caveolin-3) and Chromogenic Multiplex IHC for BOND RX/RX^{m} (Leica Microsystems, Inc.) was used as detection agent (23,24). Anti-Mouse UltraPolymer HRP (2MH-050: Anti-Mouse UltraPolymer HRP 50 ml; Cell IDx; Leica Microsystems, Inc.) was used to increase the sensitivity and signal amplification. The following primary antibodies were used: Dystrophin (dilution, 1:100; cat. no. ab275391; Abcam; 60 min at 25˚C), α-sarcoglycan (dilution, 1:1,000; cat. no. ab189254; Abcam; 60 min at 25˚C), β-sarcoglycan (dilution, 1:100; cat. no. ab135954; Abcam; 60 min at 25˚C) and caveolin-3 (dilution, 1:1,000; cat. no. ab289544; Abcam; 60 min at 25˚C). The following secondary antibody was used: Anti-Rabbit IgG H&L (HRP) (dilution, 1:2,000; cat. no. ab205718; Abcam; 10 h at 4˚C). A light microscope (total magnification, x200) was used to capture the images.

Whole exome sequencing. A blood sample was collected from the proband and genomic DNA was extracted (QIAamp DNA Blood Mini Kit; Qiagen GmbH) according to the manufacturer's instructions. The genomic DNA of the proband was subjected to whole exome sequencing (25). Illumina® DNA Prep with Exome 2.5 Enrichment (cat. No. 20025524; Illumina, Inc.) was used to prepare DNA samples for whole exome sequencing. DNA was quantified using Qubit Fluorometric Quantitation (Thermo Fisher Scientific, Inc.). The quality of DNA was assessed by 1.5% agarose gel electrophoresis and visualized by ethidium bromide with using a GelDoc Go Gel Imaging System (Bio-Rad Laboratories, Inc.). The recommended read length of whole exome sequencing was 2x150 bp. SureSelect Human All Exon v6 (cat. No. 5190-8864, Agilent Technologies, Inc.) was used to capture the sequences. The sequencing library was prepared and the enriched library was subjected to whole exome sequencing on an Illumina HighSeq4000 (HiSeq 3000/4000 SBS Kit; cat. no. FC-410-1003; Illumina, Inc.). The loading concentration of the final sequencing library was 250-300 pM as determined using the Kapa Library quantification kit (part no. KK4824; Roche Diagnostics) and size-corrected using fragment analysis. Sequencing of both the forward and reverse strands was performed (paired end). After sequencing, the alignment of sequencing reads was performed using Burrows-Wheeler Aligner software (v0.59; https://bio-bwa.sourceforge.net/). Then, local realignment of the Burrows-Wheeler-aligned reads was performed by Genome Analysis Toolkit (GATK) IndelRealigner (26). Next, base quality recalibration of the Burrows-Wheeler-aligned reads was carried out using GATK BaseRecalibrator (26). Next, single-nucleotide variants (SNV) and insertions or deletions were identified using GATK Unified Genotyper (26). Then, these variants were annotated with the Consensus Coding Sequences Database (https://www.ncbi.nlm.nih.gov/CCDS/CcdsBrowse.cgi) at the National Centre for Biotechnology Information (NCBI). Illumina pipeline was used for image analysis and base calling. In addition, indexed primers were designed and used for data fidelity surveillance. SOAP aligner (soap2.21) software (27) was used to align the clean sequencing reads with human reference genome (hg19). Lastly, to assemble the consensus sequence and call genotypes in target regions, SOAPsnp (v1.05) software (28) was used.

Bioinformatics data analysis and interpretation. Variants obtained from whole exome sequencing were collected. Variants with minor allele frequency (MAF) of <0.01 in dbSNP, HapMap, 1000 Genomes Project and our in-house database of 50,000 Chinese Han samples were selected. Public databases, namely, dbSNP (https://www.ncbi.nlm.nih.gov), HapMap (https://www.genome.gov), 1000 Genome Database (http://www.internationalgenome.org) and our in-house database for 50,000 Chinese Han samples were used (29-31). All of these databases were used to identify the MAFs of genetic variations in different populations. Using the MAF of a genetic variant in a specific population, the possible pathogenicity of this genetic variant for a specific case can be interpreted. The Human Gene Mutation database (HGMD, www.hgmd.cf.ac.uk/) contains all the reported genetic variants associated with monogenic disorders. Hence, by using this database, it can be interpreted whether the identified genetic variant is a novel or previously reported cause of any disease (32). Online Mendelian Inheritance in Man (OMIM, https://www.omim.org) is a highly comprehensive and freely available database, comprised of >16,000 human genes associated with all known Mendelian disorders (33). This database also provides information regarding genotype-phenotype correlation. Exome Aggregation Consortium (ExAC, http://exac.broadinstitute.org) contains exome sequencing data from largescale sequencing projects from different populations worldwide (34). Thus, the possible pathogenicity of identified genetic variants was confirmed by comparing their frequencies in different populations. Genome Aggregation Database (gnomAD, https://gnomad.broadinstitute.org) also comprises both genome and exome sequencing data from large-scale genome or exome sequencing projects from different populations around the world (35). Therefore, by comparing the frequencies of any reported genetic variant in different populations, the pathogenicity of the identified genetic variants in the present study was interpreted.

Variant interpretation was performed based on the variant interpretation guidelines of American College of Medical Genetics and Genomics (ACMG; Bethesda, Maryland, USA) (36). All the heterozygous, homozygous and compound heterozygous variants were selected based on gene function and disease association by OMIM and the literature. The expression of variants was confirmed using 'Mutalyzer 2.0.35' software (https://v2.mutalyzer.nl/) which strongly follows the Human Genome Variation Society guidelines (37). The whole exome sequencing quality control data are described in Table I.

Sanger sequencing. Sanger sequencing was performed to validate the possible disease-causing mutations identified by whole exome sequencing. Primers for polymerase chain reaction (PCR) were designed based on the reference genomic sequences of the Human Genome from GenBank (NCBI;

Table I. Quality control data of whole exome sequencing.

Sequencing quality control data	Value
Raw reads (mapped to hg19)	9,487,685
Raw data yield, Mb	850.26
Reads mapped to target region	5,978,717
Reads mapped to flanked 100 bp region	6,269,868
Data mapped to target region, Mb	488.78
Data mapped to flanked 100 bp region, Mb	498.98
Length of target region, bp	887,989
Length of flanked 100 bp region, bp	979,880
Number of covered bases on target region	804,587
Coverage of target region, %	99.87
Number of covered bases on flanked 100 bp region	987,890
Coverage of flanked 100 bp region, %	99.92
Average (mean) sequencing depth of target region (30X)	590.89
Average (mean) sequencing depth (30X) of flanked 100 bp region	486.98

https://www.ncbi.nlm.nih.gov/genbank/). PCR products were subjected to Sanger sequencing. Sanger sequencing data were compared and analyzed.

The heterozygous novel mutation identified through whole exome sequencing was validated by Sanger sequencing. Sanger sequencing was performed with the following primers: Forward (F)'-5'-TGGTGGAGGGAAGGGATAGG-3'; reverse (R)5'-TGGCAAAGGGACAAGGGTTT-3'; the reference sequence NM_000070 of *CAPN3* gene was used.

Reverse transcription-PCR (RT-PCR) and Sanger sequencing. In order to understand the effect of the novel splice-site mutation of the *CAPN3* gene on the splicing event of *CAPN3* mRNA, RT-PCR followed by Sanger sequencing was performed. Muscle samples were collected from the proband and their family members, and total RNA was extracted using RNAqueous™ Total RNA Isolation Kit (Thermo Fisher Scientific, Inc.) and reverse transcribed to cDNA using PrimeScript cDNA Synthesis Kit (cat. no. RR037A; Takara Biotechnology, Co., Ltd.) according to the manufacturer's recommendations. cDNA from the proband and their family members were amplified with the use of primers (F, 5'-CTG CTTCGTTAGGCTGGAGG-3'; R, 5'-GAAGCCTGTAGG GGTGTAGC-3') encompassing the coding sequence from exon 22 to exon 24. Then, the amplified cDNAs were run on a 2% agarose gel (2 g agarose powder was mixed with 100 ml 1xTAE in a microwavable flask and the gel was made). purified using DNAclear™ Purification Kit (Thermo Fisher Scientific, Inc.). Finally, Sanger sequencing was performed as aforementioned for the proband and family members and the data were analyzed.

Relative expression of CAPN3 mRNA. Reverse-transcribed cDNA was collected for fluorescence quantitative detection by quantitative (qPCR). The One-Step TB Green® PrimeScript™ RT-PCR Kit II (Perfect Real Time; cat. no. RR086A; Takara Biotechnology Co., Ltd.) was used. The thermocycling conditions were as follows: 15 min at 95˚C to activate the chemically modified hot-start Taq DNA polymerase, followed by 35-45 cycles of a 15-sec denaturation at 95˚C and 60 sec annealing and extension at 60˚C. The target gene and housekeeping gene (GAPDH; F-5'-GTCTCCTCTGACTTCAAC AGCG-3' and R-5'-ACCACCCTGTTGCTGTAGCCAA-3') of each sample were subjected to (q)PCR. The change in RNA expression based on the detected Cq value was calculated. Primers used in qPCR were as follows: *CAPN3* F, 5'-CTG CTTCGTTAGGCTGGAGG-3'; R, 5'-GAACTTACTTGA GGCATATG-3'. The RNA sample from the normal healthy individual was collected from our hospital's sample bank (The Reproductive Medicine Centre Sample Bank, The First Hospital of Lanzhou University, Lanzhou, China). The hospital's sample bank (The Reproductive Medicine Centre Sample Bank, The First Hospital of Lanzhou University, Lanzhou, China) collected the RNA sample from the normal healthy individual after getting written informed consent. Data were analysed using the comparative threshold cycle ($2^{-\Delta\Delta Cq}$) method (38).

Results

Clinical description of proband (II-1). The proband, a 16-year-old male patient from China, manifested with gradual and progressive weakness of upper and lower extremities. The clinical symptoms first appeared at 8 years old with slow, progressive weakness of muscles and an abnormal gait. At 10 years old, the proband presented with slow, progressive weakness of lower limbs with frequent falls, difficulty in standing, walking and climbing stairs. At the age of 16 years, physical testing revealed that the proband could only walk unaided for <15 min and that the proband was unable to raise their arms above their head. No sensory, ocular or bulbar abnormalities were identified, and neurological examination showed severe weakness of proximal muscles in all limbs, pelvic and shoulder girdles. At the age of 16 years, the proband had a normal mental status with no oculomotor or facial abnormalities with sensory and coordination examinations also finding no abnormalities. In the present study, bilateral atrophy of the biceps, shoulder muscles, hip adductors, posterior thigh muscles and knee flexors, as well as moderate hypertrophy on both sides of the calves and scapular winging, was reported. In order to assess muscle strength, the Medical Research Council (MRC) Scale was used (39). The MRC scale is divided into five grades (grade 5, normal muscle; grade 4, movement of the limb against gravity and resistance; grade 3, movement of the limb against gravity over the full range; grade 2, movement of the limb but not against gravity; grade 1, visible contraction without movement of the limb; grade 0, no visible contraction). There were six muscles examined (shoulder abductors, elbow flexors, wrist extensors, hip flexors, knee extensors and foot dorsiflexors) in both the upper and lower limbs on both left and right sides, each with a score from 0 to 5. Hence, the total score ranged from 60 (normal) to 0 (quadriplegic) (39). The muscle power of proximal upper and lower extremities was grade 3, while distal upper and lower extremities was 4+ according to the MRC scale. Moreover, deep tendon reflexes were normal in the proband's arm while no deep tendon reflexes were found

in their lower extremities. Gowers' sign was used to ascertain the weakness of the muscle in the pelvic girdle or proximal muscle in lower limbs (40). This sign is a medical term that describes the strength of hip and thigh muscle, and is often identified amongst patients in the advanced stages of muscular dystrophies. The presence of Gowers' sign with decreasing plantar reflexes was identified in the proband. No abnormalities were found in the nerve conduction study; however, an electromyographic study revealed chronic myopathy. Thyroid tests were in the normal range; however, laboratory tests identified highly elevated levels (4,754 IU/l; normal, 35-232 IU/l) of serum creatine kinase. Normal levels of serum lactate and transaminases were observed in the proband. No abnormalities were identified in the electrocardiogram and echocardiogram, and the pulmonary function test (PFT) was normal.

According to these aforementioned clinical presentations, the proband was clinically diagnosed with LGMD.

Proband's younger sister (II-2). The younger sister of the proband, a 14-year-old girl from China, manifested with progressive weakness of muscles since childhood. They presented with similar clinical symptoms, disease onset and progression as the proband. At 7 years old, they demonstrated difficulty standing, walking or running with frequent falls. These clinical symptoms gradually and progressively developed, and at 10 years old, they had exercise intolerance and difficulty standing from the sitting position independently. They developed weakness in both of the upper and lower extremities and finally lost the ability to ambulate independently at 11 years old. They also showed atrophy of both bilateral biceps and quadriceps with neurological examination showing weakness in the limb-girdle muscles. Their muscle strength was gradually and progressively reduced in the upper extremities of the proximal muscle, and lower extremities of both the proximal and distal muscles. Absence or diffusely reduced deep tendon reflexes were identified in the lower extremities; however, no abnormalities were found in extraocular movements and cognition. Diffuse atrophy in all upper and lower leg muscles was identified, PFT found no abnormalities, and physical and neurological examinations revealed that the muscle power of the proximal upper and lower extremities was grade 3 and 2, respectively, according to the MRC scale. The presence of Gowers' sign, as well as pelvic girdle and leg muscle atrophy, was observed; however, no abnormalities in facial muscles were identified. Laboratory tests found elevated levels (1,050 IU/l; normal, 35-232 IU/l) of serum creatine kinase; however, the levels of serum lactate and transaminases were normal. Electrocardiogram and echocardiogram showed no cardiac abnormalities, and no abnormalities were found in nerve conduction velocity.

Proband's mother (I-2). The mother of the proband was a 42-year-old woman from China that presented with gradual, progressive weakness, and atrophy of both proximal and distal muscles. At 14 years old, they presented with difficulty running, climbing stairs, standing up from a sitting position and a waddling gait. At 18 years old, they struggled to walk independently and lift weights, and by their early twenties, they had lost the ability to walk independently, showing a complete loss of ambulation. They had an unremarkable medical history with normal sensation, no intellectual disabilities, and had never been reported to have fasciculations or pseudo-hypertrophy of calf muscles or joint contractures. However, neurological examination showed weakness and atrophy of limb-girdle muscles and an absence of all deep tendon reflexes. Laboratory tests found elevated levels (2,000 IU/l; normal, 35-232 IU/l) of serum creatine kinase. No abnormalities were identified in the levels of serum lactate and transaminases. The muscle power of both proximal upper and lower extremities, and distal upper and lower extremities were grade 2 according to the MRC scale, and the presence of Gowers' sign with atrophy of limb-girdle muscles was identified. No cardiac, motor or sensory nerve conduction abnormalities were identified; however, typical myopathic right biceps, severe atrophy of lower limbs and atrophy of paraspinal muscle were identified. At 30 years old, they developed back pain, hyperlordosis and myalgia, and both their proximal limb and abdominal wall muscles became weak. At present, they have manifested with paraspinal muscle atrophy.

Magnetic resonance imaging (MRI) of the muscle. MRI of the muscles of the proband was performed. The MRI revealed significant involvement of adductor magnus, thigh muscles (biceps femoris, semimembranosus and semitendinosus) and calf muscles (gastrocnemius and soleus) (Fig. 1B-E). Hypertrophy of the gracilis was detected; however, normal appearance of the rectus femoris, quadriceps femoris and sartorius of the thigh muscle was identified. Moreover, normal appearance of the tibialis anterior, tibialis posterior and extensor digitorum longus of the calf muscle was reported.

Clinical descriptions of the proband, their younger sister and mother have been comprehensively summarized in Table II.

Muscle biopsy pathology. Muscle biopsies of the proband showed mild to moderate dystrophic changes with H&E staining (Fig. 1F). These changes included increased fiber size variation with scattered atrophic and hypertrophic fibers, necrotic fibers undergoing myophagocytosis, grouped regeneration, endomysial fibrosis and fatty replacement (Fig. 1F). NADH staining revealed the mildly disorganized structure of the intermyofibrillar network (Fig. 1G) The immunostaining of caveolin-3, dystrophin, α-sarcoglycan and β-sarcoglycan indicated normal expression (positive staining) (Fig. 1H-K).

According to the aforementioned clinical symptoms and test results, the clinical diagnosis, therapeutic interventions and disease management were confirmed for the studied family.

Identification of a novel mutation in the CAPN3 gene. Whole exome sequencing and Sanger sequencing identified a novel heterozygous splice-acceptor site mutation (c.2440-1G>A) in intron 23 of the *CAPN3* gene in the proband. Sanger sequencing confirmed that this heterozygous novel mutation was also present in the mother and younger sister of the proband, while the father did not harbor the mutation (Fig. 1L).

The mutation was not present in 100 ethnically-matched normal healthy controls from our in-house database. This previously generated in-house control database collected genomic DNA samples from 100 normal healthy individuals, after getting their written informed consent, and performed whole exome sequencing to obtain raw sequencing data, followed by bioinformatics data analysis and interpretation.

Table II. Clinical characteristics of the proband, their younger sister and mother.

Clinical characteristics	Proband (II-1)	Proband's younger sister (II-2)	Proband's mother (I-2)
Age, years	16	14	42
Sex	Male	Female	Female
Age of onset, years	8	7	14
Clinical symptoms	Difficulty in standing, walking, climbing stairs, walking unaided for <15 min and inability to raise arms above head.	Difficulty in standing, walking, climbing stairs or running with frequent falls, exercise intolerance, and difficulty rising from the floor or standing from the sitting position independently.	Difficulty in running, climbing stairs, walking independently, lifting weights, standing up from sitting position and a waddling gait.
Neurological examination	Severe weakness of the proximal muscles of all limbs, pelvic and shoulder girdles.	Weakness and atrophy of limb-girdle muscles.	Weakness and atrophy of limb-girdle muscles.
Muscle weakness and atrophy	Bilateral atrophy of the biceps, shoulder muscles, hip adductors, posterior thigh muscles and knee flexors and moderate hypertrophy on both sides of the calves and scapular winging.	Diffuse atrophy in all upper and lower leg muscles.	Typical myopathic right biceps, severe atrophy of lower limbs and atrophy of paraspinal muscle, back pain, hyperlordosis and myalgia.
Muscle power (MRC Scale)	Proximal upper and lower extremities were grade 3, while distal upper and lower extremities were 4+.	Proximal upper and lower extremities and proximal lower extremities were grade 3 and 2, respectively.	Proximal upper and lower extremities were grade 2, and distal upper and lower extremities were grade 2.
Deep tendon reflexes	Normal in arms; absent in lower extremities	Absent or diffusely reduced in lower extremities.	Absent of all.
Gowers' sign	Present with decreasing plantar reflexes.	Present with pelvic girdle and leg muscle atrophy.	Present with limb-girdle muscle atrophy.
Creatine kinase levels, IU/l	4,754	1,050	2,000

MRC, medical research council.

This normal control database has been used as a reference database, thus if any novel variant is identified in any gene, we can compare whether it is already present in the in-house database in order to understand its pathogenicity. This mutation was also absent in the HGMD, OMIM, ExAC, dbSNP, gnomAD and 1000 Genome Database, as well as our in-house database, which consists of ~50,000 Chinese Han samples.

The mutation (c.2440-1G>A) is classified as 'likely pathogenic' [absent in population database (PM2) + predicted null variant in a gene where loss-of-function is a known mechanism of disease (PVS1) + co-segregation of disease in multiple affected family members (PP1)] according to the variant interpretation guidelines of ACMG (36). The mutation (c.2440-1G>A) is co-segregated with the disease phenotype in this family with an autosomal dominant mode of inheritance.

Functional characterization of the novel splice-acceptor site mutation. Individuals with wild-type (father of the proband) and mutated (proband, their mother and younger sister) *CAPN3* underwent PCR for amplification of *CAPN3* cDNA encompassing the coding sequence (exon 22-24), which was run on a 2% agarose gel. A 200-bp band for wild-type *CAPN3* cDNA was found, whereas a 176-bp band for mutated *CAPN3* cDNA was identified (Fig. 2A).

Sanger sequencing of mutated cDNA from the proband, their mother and younger sister revealed that the mutation (c.2440-1G>A) at the last nucleotide of intron 23 of the *CAPN3* gene disrupts the wild-type *CAPN3* exon 24 splice acceptor-site and leads to aberrant splicing of *CAPN3* mRNA, finally resulting in the skipping of exon 24 (24 bp). Complete loss of exon 24 causes the formation of a truncated CAPN3 protein (p.Trp814*) with the removal of eight amino acids from the C-terminal (Fig. 2B). However, Sanger sequencing of the wild-type *CAPN3* cDNA showed normal splicing of exon 22 to exon 24 (Fig. 2B). The splicing mechanism of both wild-type and mutated cDNA is schematically presented (Fig. 2C).

Relative expression of CAPN3 mRNA determined by RT-qPCR. Relative expression levels of *CAPN3* mRNA revealed a significantly decreased mutated *CAPN3* transcript level in the proband, their younger sister and mother while the father of the proband showed normal expression (same as the normal healthy

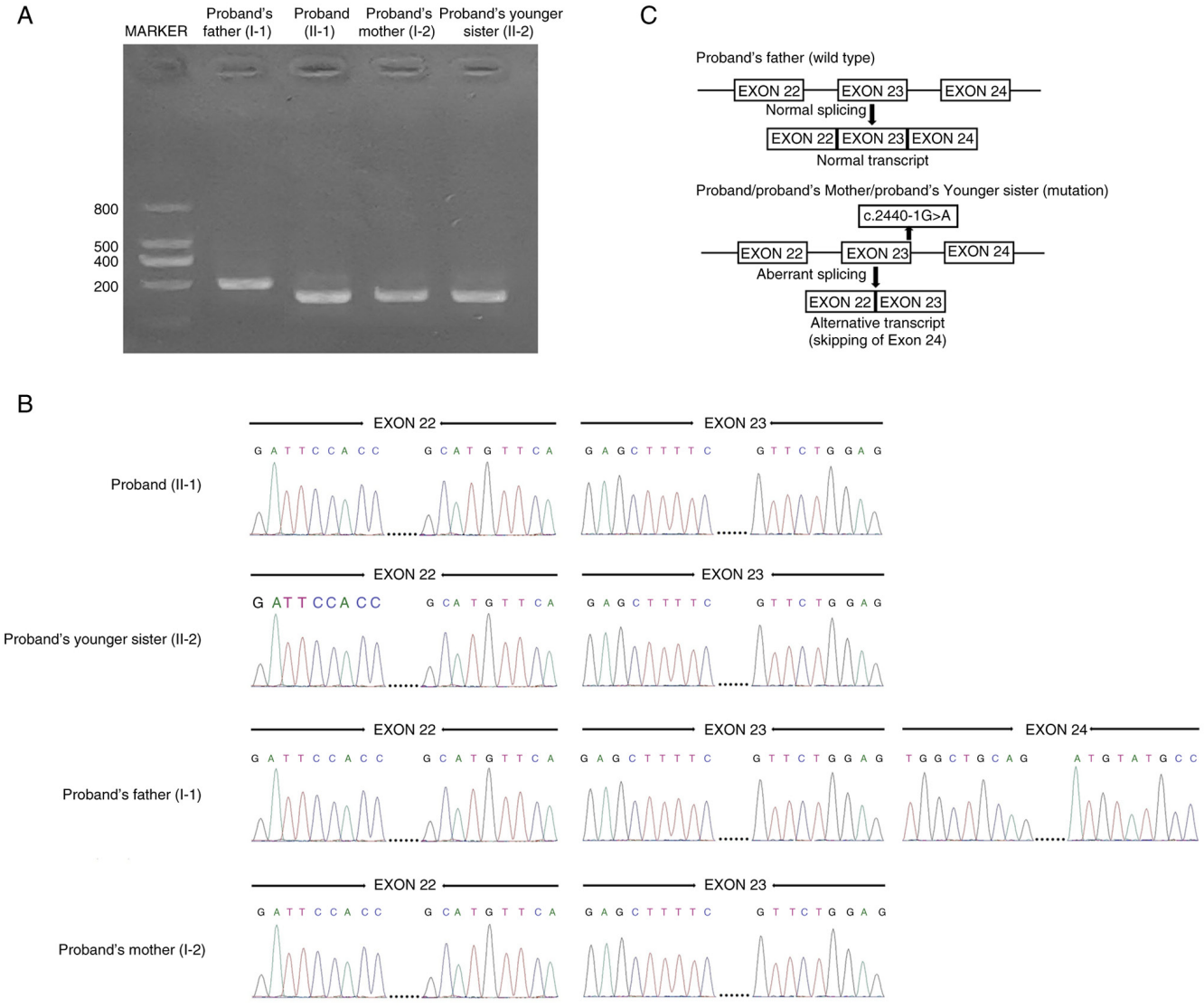

Figure 2. (A) cDNA gel electrophoresis (left to right): Lane 1: DNA molecular marker (200-800 bp); lane 2: Wild-type or normal *CAPN3* cDNA (proband's father); lane 3-5: Mutated *CAPN3* cDNA (proband, proband's younger sister, proband's mother). (B) Sequencing result of normally spliced wild-type or normal *CAPN3* cDNA (proband's father) showing only exons 22, 23 and 24. Sequencing results of the aberrantly spliced mutated *CAPN3* cDNA (proband, proband's younger sister, proband's mother) showing only exons 22 and 23 (complete loss of exon 24). (C) Schematic presentation of the splicing event of both wild type and mutated *CAPN3* cDNA. *CAPN3*, calpain 3.

control individual) of wild-type CAPN3 mRNA (Fig. 3). These results also suggested that the mutant CAPN3 transcript (proband, proband's mother and younger sister) was present at detectable levels. Therefore, the mutated CAPN3 transcript was not degraded by the nonsense-mediated mRNA decay pathway.

All 24 exons of the *CAPN3* gene are schematically presented in Fig. 4A, and the mutation is located at the last nucleotide of exon 23. The wild type CAPN3 protein structure is shown in Fig. 4B. The mutated CAPN3 protein (with complete loss of exon 24) is presented in Fig. 4C. According to the structural point of view, this mutation causes partial loss of domain IV of the CAPN3 protein, which is involved in calcium binding and homodimerization (41).

Discussion

In the present study, a nonconsanguineous family from China clinically diagnosed with LGMDD4 was investigated and analyzed. The proband (II-1), their mother (I-2) and younger sister (II-2) were clinically diagnosed with LGMDD4, while the father of the proband (I-1) was phenotypically normal. Whole exome sequencing identified a novel heterozygous splice-acceptor site mutation (c.2440-1G>A) in the *CAPN3* gene in the proband. Sanger sequencing confirmed that the mother and younger sister of the proband were also carriers of this mutation, while the father was devoid of it. This splice-site mutation causes aberrant splicing of CAPN3 mRNA, leading to the complete loss of exon 24, finally resulting in the formation of a truncated (p.Trp814*) CAPN3 protein of 813 amino acids, hence, it is a loss-of-function mutation. The proband, the mother and the younger sister had mutations in the *CAPN3* gene (as established by whole exome sequencing and Sanger sequencing). Thus, the CAPN3 mRNA expression in the proband, sister and mother was expression of the mutated CAPN3. The mutated CAPN3 mRNA showed significantly reduced expression compared with the wild-type CAPN3

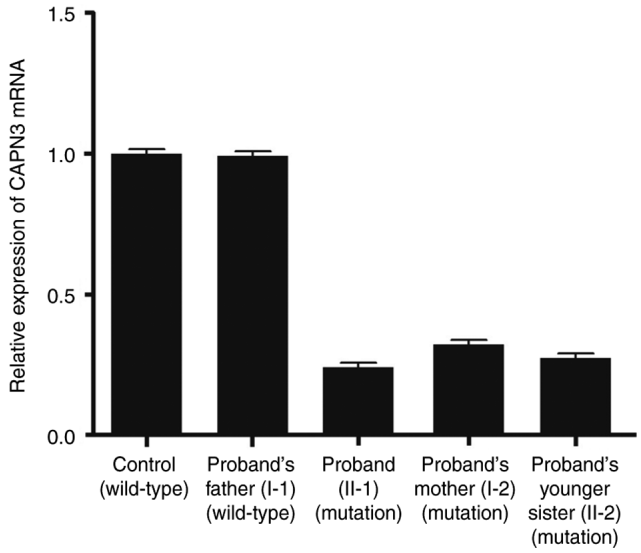

Figure 3. Relative expression of CAPN3 mRNA by quantitative polymerase chain reaction. Relative expression of CAPN3 mRNA revealed a decreased mutated CAPN3 transcript level in the proband, their younger sister and mother, while the proband's father showed normal expression of wild-type CAPN3 mRNA. The comparative threshold cycle ($2^{-\Delta\Delta Cq}$) method was used to determine the relative expression levels of the wild-type and mutated CAPN3 mRNA. *CAPN3*, calpain 3.

mRNA. This mutation causes both structural and functional changes in CAPN3 protein, which lead to LGMDD4 in the proband and all affected family members. In the present study, other pathogenic or likely pathogenic variants in other genes associated with muscular dystrophies were not identified. In addition, no other variants in genes (titin, dysferlin, filamin C and *ATP2A2*) that interact with *CAPN3* were identified; therefore, a very rare form of LGMDD4 in a Chinese family was reported in the present study.

The patients in the present study showed comparatively milder phenotypes than that of previously reported patients with LGMDD4 (15-17). Additionally, intrafamilial phenotypic variability was identified in this family with the level of serum creatine kinase not showing an association with disease severity. This is in line with the literature, as some patients with LGMDD4 are reported to have normal serum creatine kinase during their clinical course, while others have elevated levels of serum creatine kinase (42).

It has previously been reported that CAPN3 interacts with tropomyosin, α-actinin-3 and LIM-domain binding protein 3 (14,43). CAPN3 strongly interacts with ryanodine receptor type 1 (RyR1), calsequestrin and sarco/endoplasmic reticulum calcium ATPase proteins to maintain calcium homeostasis (43-45). In addition, CAPN3 increases the activity of NCX3, which also regulates calcium homeostasis (46). Maintenance and remodeling of sarcomeres is regulated by CAPN3 and titin, and CAPN3 is also involved in modulating the function of mitochondria (45,46). Germline mutations in the *CAPN3* gene lead to the formation of non-functional CAPN3 protein, which in turn causes reduced expression of RyR1 and reduced release of calcium from the sarcoplasmic reticulum, thus finally resulting in the dysregulation of calcium homeostasis and manifesting as LGMDD4 (45-47). Additionally, reduced expression of RyR1 and calcium/calmodulin-dependent kinase II signaling has already been reported in muscles among patients with LGMDD4 (48). Hence, this is the pathophysiological mechanism underlying the disease phenotype among patients with LGMDD4. The pathophysiological mechanism of CAPN3-associated LGMDD4 is associated with the NF-κB pathway (49). CAPN3 activates NF-κB by calcium-dependent degradation of IκBα, a NF-κB inhibitor. Activated NF-κB causes degradation of protein, inflammation and fibrosis of skeletal muscle (49). Therefore, mutations in the *CAPN3* gene lead to dysregulation of the NF-κB pathway and could be the pathophysiological mechanism for LGMDD4. Additionally, the ubiquitin-proteasome system (UPS) and the autophagy-lysosome pathway are, reportedly, involved in the proteolytic processes of cell regulatory turnover of protein in muscles. It has been reported that the UPS is a main pathway leading to muscle atrophy (49,50).

At present, ~20 different types of LGMD have been reported with extreme intra- and inter-familial phenotypic heterogeneity, even among patients with the same LGMD subtype (51,52). Assessing the serum creatine kinase level or analyzing electrical activity of the muscle is the key point of clinical diagnosis of muscular disorders; however, diagnosing the exact type of muscular disorder is the biggest challenge at present (53). Clinical diagnosis of calpainopathies is usually achieved through muscle biopsy, to measure the presence of CAPN3 in the muscle (54). Immunohistochemical staining is not a simple or confirmatory diagnostic procedure for patients with calpainopathies because of the rapid autolysis of CAPN3 (41). Several types of LGMD have been identified with overlapping clinical symptoms, and genetic testing is the most efficient way to ensure accurate and timely clinical diagnosis. Hence, genetic molecular diagnosis through whole exome sequencing is the most easy, useful, accurate, and least time-consuming method for clinical diagnosis of this disease (41).

Among all the reported mutations of the *CAPN3* gene associated with LGMD, the majority are missense mutations (60-70%) (55,56). Most of the mutations in the *CAPN3* gene are located in exons 1, 4, 5, 8, 10, 11 and 21 (57,58). At present, ~300 mutations of *CAPN3* have been reported and according to the location of these mutations, *CAPN3* gene consists of two hotspots, one on exon 11 and the other on exon 21. Among these reported mutations, some are founder but the majority are private variants (53,59,60). Duguez *et al* (61) described the first study, which involved 548 patients with myopathy, including LGMD, from 181 families and 19 countries, and reported 97 pathogenic mutations of the *CAPN3* gene (62).

Structurally, the CAPN3 protein is comprised of four domains. Domain I is an N-terminal domain containing the nuclear localization signal. Germline mutations located in domain I cause a loss of the nuclear transport function of CAPN3 (41). Domain II (IIa, IS1 and IIb) is an evolutionarily conserved cysteine protease domain, which is involved in protease activity. Mutations in domain II causes a loss of the protease activity of CAPN3 (49). Domain III is directly responsible for structural changes of activated CAPN3. Mutations occurring in domain III lead to no structural changes in CAPN3 upon its activation (43). Lastly, domain IV is majorly involved in calcium ion (Ca^{2+}) binding and homodimerization of CAPN3. Germline mutations in domain IV cause formation

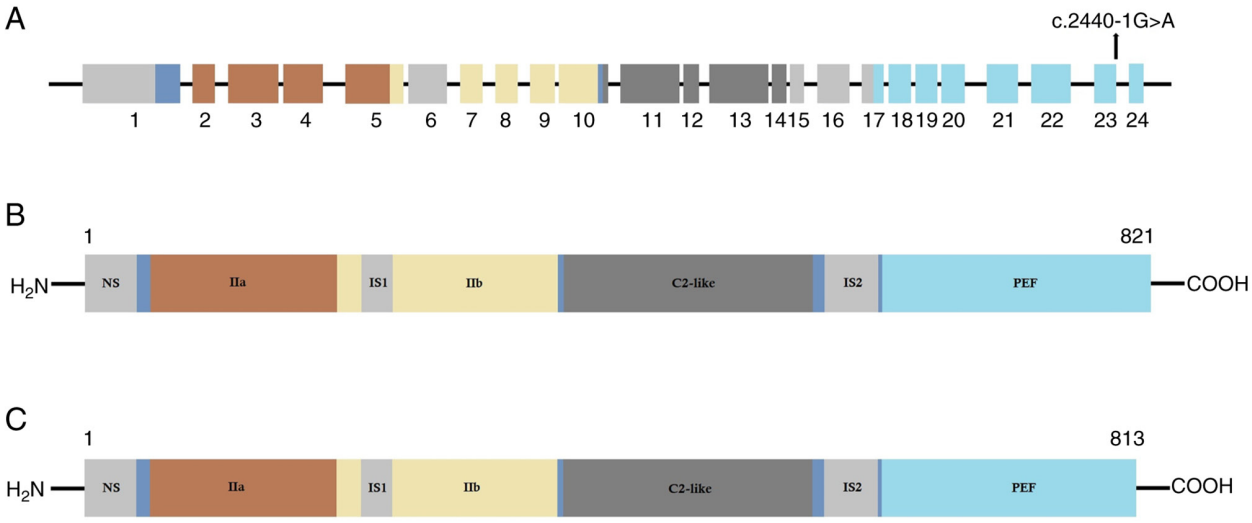

Figure 4. Structure of *CAPN3* gene, wild-type and mutated CAPN3 proteins. (A) *CAPN3* gene contains 24 exons. Location of the splice site (c.2440-1G>A) mutation is indicated. (B) Wild-type CAPN3 protein is a multidomain protease with 821 amino acids. (C) Mutated CAPN3 protein comprised of 813 amino acids with partial loss of domain IV (PEF domain). CAPN3, calpain 3.

of non-functional CAPN3, which is unable to bind with Ca^{2+} and lacks the ability to homodimerize (46). Hence, these mutations located in different domains of *CAPN3* gene can cause LGMDD4 (50).

At present, several gene therapy-based strategies have been used to treat patients with LGMDD4 that harbor a *CAPN3* mutation. Moreover, cellular therapies, drug therapies (glucocorticoid treatment) or gene therapies (AAV-mediated therapy and CRISPR-Cas9 gene editing) have been performed either in preclinical or clinical phases; however, there is no cure (63). Endoplasmic reticulum stress factor-targeting inhibitors and small molecules (tauroursodeoxycholic acid, salubrinal and rapamycin) have also been considered as potential therapeutic strategies (11). However, at present, no therapeutic strategies have been developed to treat the progressive muscle loss and premature death of patients with LGMD (64). In the present study, a single interesting case of *CAPN3*-associated LGMDD4 was reported. A limitation of the study is that due to the unavailability of fresh muscle samples, western blotting to confirm the relative expression of CAPN3 protein among the proband and all affected family members could not be performed. In the future, more cases of *CAPN3*-associated LGMDD4 should be analyzed and reported on in order to understand the disease mechanism, genotype-phenotype correlation and possible clinical management for the patients.

In conclusion, in the present study, a 16-year-old male patient from China with gradual and progressive weakness, and atrophy of the muscles in both the legs was reported on. The younger sister and mother of the proband displayed similar clinical symptoms as the proband. Whole exome sequencing identified a heterozygous novel splice-site mutation (c.2440-1G>A) in intron 23 of the *CAPN3* gene in the proband. This mutation causes aberrant splicing of *CAPN3* mRNA and leads to the skipping of exon 24 and, finally, results in the formation of a truncated (p.Trp814*) CAPN3 protein. To the best of our knowledge, the present study is the first to report on a case of *CAPN3* gene-associated LGMDD4 in the Chinese population.

Acknowledgements

Not applicable.

Funding

This study is supported by the Key Research and Development Plan of Gansu Province (grant no. 21YF1FA115), Key Research and Development Plan of Gansu Province in 2022 (grant no. 22YF7FA084) and Natural Science Foundation of Gansu Province in 2022 (grant no. 22JR5RA911).

Availability of data and materials

The datasets generated and/or analyzed during the current study are not available to patient privacy but are available from the corresponding author on reasonable request.

Authors' contributions

BM, JY, XJ, LihZ and XM were responsible for the clinical investigation (radiology, histology and immunohistochemistry) for the proband and his family members. XS and LilZ performed genetic analysis. BM, JY, XZ and XM performed clinical investigation. SB, LilZ and XM were responsible for project administration. BM, JY, XJ, LihZ and XM acquired materials. SB, LilZ and XM supervised the present study; BM, JY, XJ, SB, LihZ and XM wrote the original draft. SB, LilZ and XM wrote, reviewed and edited the manuscript. LilZ and XM confirm the authenticity of all the raw data. All authors read and approved the final manuscript.

Ethics approval and consent to participate

The ethics committee of The Reproductive Medicine Centre, The First Hospital of Lanzhou University approved the present study (approval no. 2021-A-8900920; Lanzhou, China) in accordance with the recommendations of The Declaration

of Helsinki. Written informed consent was obtained from all family members and the parents of the minor patients for their participation in this study. The genomic DNA samples from the 100 normal healthy individuals were collected from our hospital's sample bank (The Reproductive Medicine Centre Sample Bank, The First Hospital of Lanzhou University, Lanzhou, China). The hospital's sample bank (The Reproductive Medicine Centre Sample Bank, The First Hospital of Lanzhou University, Lanzhou, China) collected the genomic DNA samples from the 100 normal healthy individuals after obtaining written informed consent. The ethics committee of The Reproductive Medicine Centre, The First Hospital of Lanzhou University (approval no. 2021-C-723149; Lanzhou, China) approved the use of the genomic DNA samples from 100 normal healthy individuals from the hospital's sample bank (The Reproductive Medicine Centre Sample Bank, The First Hospital of Lanzhou University, Lanzhou, China) for the present study. The RNA sample from the normal healthy individual was collected from our hospital's sample bank (The Reproductive Medicine Centre Sample Bank, The First Hospital of Lanzhou University, Lanzhou, China). The hospital's sample bank (The Reproductive Medicine Centre Sample Bank, The First Hospital of Lanzhou University, Lanzhou, China) collected the RNA sample from the normal healthy individual after getting written informed consent. The ethics committee of The Reproductive Medicine Centre, The First Hospital of Lanzhou University (approval no. 2021-C-934572; Lanzhou, China) approved the use of the RNA sample from a normal healthy individual from the hospital's sample bank (The Reproductive Medicine Centre Sample Bank, The First Hospital of Lanzhou University, Lanzhou, China) for the present study.

Patient consent for publication

Written informed consent was obtained from all family members and the parents of the minor patients for the publication of this study.

Competing interests

The authors declare that they have no competing interests.

References

1. Allamand V, Broux O, Richard I, Fougerousse F, Chiannilkulchai N, Bourg N, Brenguier L, Devaud C, Pasturaud P, Pereira de Souza A, *et al*: Preferential localization of the limb-girdle muscular dystrophy type 2A gene in the proximal part of a 1-cM 15q15.1-q15.3 interval. Am J Hum Genet 56: 1417-1430, 1995.
2. Bushby KM: Diagnostic criteria for the limb-girdle muscular dystrophies: Report of the ENMC consortium on limb-girdle dystrophies. Neuromuscul Disord 5: 71-74, 1995.
3. Wang CH, Liang WC, Minami N, Nishino I and Jong YJ: Limb-girdle muscular dystrophy type 2A with mutation in CAPN3: The first report in Taiwan. Pediatr Neonatol 56: 62-65, 2015.
4. Zheng J, Xu X, Zhang X, Wang X, Shu J and Cai C: Variants of CAPN3 cause limb-girdle muscular dystrophy type 2A in two Chinese families. Exp Ther Med 21: 104, 2021.
5. Richard I, Broux O, Allamand V, Fougerousse F, Chiannilkulchai N, Bourg N, Brenguier L, Devaud C, Pasturaud P, Roudaut C, *et al*: Mutations in the proteolytic enzyme calpain 3 cause limb-girdle muscular dystrophy type 2A. Cell 81: 27-40, 1995.
6. Feng X, Luo S, Li J, Yue D, Xi J, Zhu W, Gao X, Guan X, Lu J, Liang Z and Zhao C: Fatty infiltration evaluation and selective pattern characterization of lower limbs in limb-girdle muscular dystrophy type 2A by muscle magnetic resonance imaging. Muscle Nerve 58: 536-541, 2018.
7. Mercuri E, Bushby K, Ricci E, Birchall D, Pane M, Kinali M, Allsop J, Nigro V, Sáenz A, Nascimbeni A, *et al*: Muscle MRI findings in patients with limb girdle muscular dystrophy with calpain 3 deficiency (LGMD2A) and early contractures. Neuromuscul Disord 15: 164-171, 2005.
8. Richard I, Brenguier L, Dinçer P, Roudaut C, Bady B, Burgunder JM, Chemaly R, Garcia CA, Halaby G, Jackson CE, *et al*: Multiple independent molecular etiology for limb-girdle muscular dystrophy type 2A patients from various geographical origins. Am J Hum Genet 60: 1128-1138, 1997.
9. Groen EJ, Charlton R, Barresi R, Anderson LV, Eagle M, Hudson J, Koref MS, Straub V and Bushby KM: Analysis of the UK diagnostic strategy for limb girdle muscular dystrophy 2A. Brain 130: 3237-3249, 2007.
10. Vissing J, Barresi R, Witting N, Van Ghelue M, Gammelgaard L, Bindoff LA, Straub V, Lochmüller H, Hudson J, Wahl CM, *et al*: A heterozygous 21-bp deletion in CAPN3 causes dominantly inherited limb girdle muscular dystrophy. Brain 139: 2154-2163, 2016.
11. Richard I, Roudaut C, Saenz A, Pogue R, Grimbergen JE, Anderson LV, Beley C, Cobo AM, de Diego C, Eymard B, *et al*: Calpainopathy-a survey of mutations and polymorphisms. Am J Hum Genet 64: 1524-1540, 1999.
12. Kramerova I, Kudryashova E, Venkatraman G and Spencer MJ: Calpain 3 participates in sarcomere remodeling by acting upstream of the ubiquitin-proteasome pathway. Hum Mol Genet 14: 2125-2134, 2005.
13. Ermolova N, Kudryashova E, DiFranco M, Vergara J, Kramerova I and Spencer MJ: Pathogenity of some limb girdle muscular dystrophy mutations can result from reduced anchorage to myofibrils and altered stability of calpain 3. Hum Mol Genet 20: 3331-3345, 2011.
14. Taveau M, Bourg N, Sillon G, Roudaut C, Bartoli M and Richard I: Calpain 3 is activated through autolysis within the active site and lyses sarcomeric and sarcolemmal components. Mol Cell Biol 23: 9127-9135, 2003.
15. Martinez-Thompson JM, Niu Z, Tracy JA, Moore SA, Swenson A, Wieben ED and Milone M: Autosomal dominant calpainopathy due to heterozygous CAPN3 C.643_663del21. Muscle Nerve 57: 679-683, 2018.
16. Cerino M, Campana-Salort E, Salvi A, Cintas P, Renard D, Morales RJ, Tard C, Leturcq F, Stojkovic T, Bonello-Palot N, *et al*: Novel CAPN3 variant associated with an autosomal dominant calpainopathy. Neuropathol Appl Neurobiol 46: 564-578, 2020.
17. González-Mera L, Ravenscroft G, Cabrera-Serrano M, Ermolova N, Domínguez-González C, Arteche-López A, Soltanzadeh P, Evesson F, Navas C, Mavillard F, *et al*: Heterozygous CAPN3 missense variants causing autosomal-dominant calpainopathy in seven unrelated families. Neuropathol Appl Neurobiol 47: 283-296, 2021.
18. Sáenz A and López de Munain A: Dominant LGMD2A: Alternative diagnosis or hidden digenism? Brain 140: e7, 2017.
19. Vissing J and Duno M: Reply: Dominant LGMD2A: Alternative diagnosis or hidden digenism? Brain 140: e8, 2017.
20. Cotta A, Carvalho E, da-Cunha-Júnior AL, Valicek J, Navarro MM, Junior SB, da Silveira EB, Lima MI, Cordeiro BA, Cauhi AF, *et al*: Muscle biopsy essential diagnostic advice for pathologists. Surg Exp Pathol 4: 3, 2021.
21. Wang C, Yue F and Kuang S: Muscle histology characterization using H&E staining and muscle fiber type classification using immunofluorescence staining. Bio Protoc 7: e2279, 2017.
22. Nix JS and Moore SA: What every neuropathologist needs to know: The muscle biopsy. J Neuropathol Exp Neurol 79: 719-733, 2020.
23. Suriyonplengsaeng C, Dejthevaporn C, Khongkhatithum C, Sanpapant S, Tubthong N, Pinpradap K, Srinark N and Waisayarat J: Immunohistochemistry of sarcolemmal membrane-associated proteins in formalin-fixed and paraffin-embedded skeletal muscle tissue: A promising tool for the diagnostic evaluation of common muscular dystrophies. Diagn Pathol 12: 19, 2017.
24. Danielsson O and Häggqvist B: Skeletal muscle immunohistochemistry of acquired and hereditary myopathies. Curr Opin Rheumatol 33: 529-536, 2021.

25. Zhang R, Chen S, Han P, Chen F, Kuang S, Meng Z, Liu J, Sun R, Wang Z, He X, *et al*: Whole exome sequencing identified a homozygous novel variant in CEP290 gene causes Meckel syndrome. J Cell Mol Med 24: 1906-1916, 2020.
26. Van der Auwera GA, Carneiro M, Hartl C, Poplin R, del Angel G, Levy-Moonshine A, Jordan T, Shakir K, Roazen D, Thibault J, *et al*: From FastQ data to high confidence variant calls: The genome analysis toolkit best practices pipeline. Curr Protoc Bioinformatics: Mar 15, 2018 (Epub ahead of print). doi: 10.1002/0471250953.bi1110s43.
27. Gu S, Fang L and Xu X: Using SOAPaligner for short reads alignment. Curr Protoc Bioinformatics 44: 11.11.1-17, 2013.
28. Li R, Yu C, Li Y, Lam TW, Yiu SM, Kristiansen K and Wang J: SOAP2: An improved ultrafast tool for short read alignment. Bioinformatics 25: 1966-1967, 2009.
29. Sherry ST, Ward MH, Kholodov M, Baker J, Phan L, Smigielski EM and Sirotkin K: dbSNP: The NCBI database of genetic variation. Nucleic Acids Res 29: 308-311, 2001.
30. Clark AG, Hubisz MJ, Bustamante CD, Williamson SH and Nielsen R: Ascertainment bias in studies of human genome-wide polymorphism. Genome Res 15: 1496-1502, 2005.
31. 1000 Genomes Project Consortium; Auton A, Brooks LD, Durbin RM, Garrison EP, Kang HM, Korbel JO, Marchini JL, McCarthy S, McVean GA and Abecasis GR: A global reference for human genetic variation. Nature 526: 68-74, 2015.
32. Stenson PD, Ball EV, Mort M, Phillips AD, Shiel JA, Thomas NST, Abeysinghe S, Krawczak M and Cooper DN: Human gene mutation database (HGMD): 2003 Update. Hum Mutat 21: 577-581, 2003.
33. Hamosh A, Scott AF, Amberger JS, Bocchini CA and McKusick VA: Online mendelian inheritance in man (OMIM), a knowledgebase of human genes and genetic disorders. Nucleic Acids Res 33: D514-D517, 2005.
34. Karczewski KJ, Weisburd B, Thomas B, Solomonson M, Ruderfer DM, Kavanagh D, Hamamsy T, Lek M, Samocha KE, Cummings BB, *et al*: The ExAC browser: Displaying reference data information from over 60 000 exomes. Nucleic Acids Res 45 (D1): D840-D845, 2017.
35. Karczewski KJ, Francioli LC, Tiao G, Cummings BB, Alföldi J, Wang Q, Collins RL, Laricchia KM, Ganna A, Birnbaum DP, *et al*: The mutational constraint spectrum quantified from variation in 141,456 humans. Nature 581: 434-443, 2020.
36. Richards S, Aziz N, Bale S, Bick D, Das S, Gastier-Foster J, Grody WW, Hegde M, Lyon E, Spector E, *et al*: Standards and guidelines for the interpretation of sequence variants: A joint consensus recommendation of the American college of medical genetics and genomics and the association for molecular pathology. Genet Med 17: 405-424, 2015.
37. Lefter M, Vis JK, Vermaat M, den Dunnen JT, Taschner PEM and Laros JFJ: Mutalyzer 2: Next generation HGVS nomenclature checker. Bioinformatics 37: 2811-2817, 2021.
38. Livak KJ and Schmittgen TD: Analysis of relative gene expression data using real-time quantitative PCR and the 2(-Delta Delta C(T)) method. Methods 25: 402-408, 2001.
39. Vanhoutte EK, Faber CG, van Nes SI, Jacobs BC, van Doorn PA, van Koningsveld R, Cornblath DR, van der Kooi AJ, Cats EA, van den Berg LH, *et al*: Modifying the medical research council grading system through Rasch analyses. Brain 135: 1639-1649, 2012.
40. Chang RF and Mubarak SJ: Pathomechanics of Gowers' sign: A video analysis of a spectrum of Gowers' maneuvers. Clin Orthop Relat Res 470: 1987-1991, 2012.
41. Partha SK, Ravulapalli R, Allingham JS, Campbell RL and Davies PL: Crystal structure of calpain-3 penta-EF-hand (PEF) domain-a homodimerized PEF family member with calcium bound at the fifth EF-hand. FEBS J 281: 3138-3149, 2014.
42. Gallardo E, Saenz A and Illa I: Limb-girdle muscular dystrophy 2A. Handb Clin Neurol 101: 97-110, 2011.
43. Huang Y, de Morrée A, van Remoortere A, Bushby K, Frants RR, den Dunnen JT and van der Maarel SM: Calpain 3 is a modulator of the dysferlin protein complex in skeletal muscle. Hum Mol Genet 17: 1855-1866, 2008.
44. Toral-Ojeda I, Aldanondo G, Lasa-Elgarresta J, Lasa-Fernández H, Fernández-Torrón R, López de Munain A and Vallejo-Illarramendi A: Calpain 3 deficiency affects SERCA expression and function in the skeletal muscle. Expert Rev Mol Med 18: e7, 2016.
45. Jahnke VE, Peterson JM, Van Der Meulen JH, Boehler J, Uaesoontrachoon K, Johnston HK, Defour A, Phadke A, Yu Q, Jaiswal JK and Nagaraju K: Mitochondrial dysfunction and consequences in calpain-3-deficient muscle. Skelet Muscle 10: 37, 2020.
46. Chen L, Tang F, Gao H, Zhang X, Li X and Xiao D: CAPN3: A muscle-specific calpain with an important role in the pathogenesis of diseases (review). Int J Mol Med 48: 203, 2021.
47. Lasa-Elgarresta J, Mosqueira-Martín L, González-Imaz K, Marco-Moreno P, Gerenu G, Mamchaoui K, Mouly V, López de Munain A and Vallejo-Illarramendi A: Targeting the ubiquitin-proteasome system in limb-girdle muscular dystrophy with CAPN3 mutations. Front Cell Dev Biol 10: 822563, 2022.
48. Kramerova I, Torres JA, Eskin A, Nelson SF and Spencer MJ: Calpain 3 and CaMKIIβ signaling are required to induce HSP70 necessary for adaptive muscle growth after atrophy. Hum Mol Genet 27: 1642-1653, 2018.
49. Lasa-Elgarresta J, Mosqueira-Martín L, Naldaiz-Gastesi N, Sáenz A, López de Munain A and Vallejo-Illarramendi A: Calcium mechanisms in limb-girdle muscular dystrophy with CAPN3 mutations. Int J Mol Sci 20: 4548, 2019.
50. Place N, Ivarsson N, Venckunas T, Neyroud D, Brazaitis M, Cheng AJ, Ochala J, Kamandulis S, Girard S, Volungevičius G, *et al*: Ryanodine receptor fragmentation and sarcoplasmic reticulum Ca^{2+} leak after one session of high-intensity interval exercise. Proc Natl Acad Sci USA 112: 15492-15497, 2015.
51. Mitsuhashi S and Kang PB: Update on the genetics of limb girdle muscular dystrophy. Semin Pediatr Neurol 19: 211-218, 2012.
52. Guglieri M, Magri F, D'Angelo MG, Prelle A, Morandi L, Rodolico C, Cagliani R, Mora M, Fortunato F, Bordoni A, *et al*: Clinical, molecular, and protein correlations in a large sample of genetically diagnosed Italian limb girdle muscular dystrophy patients. Hum Mutat 29: 258-266, 2008.
53. Balci B, Aurino S, Haliloglu G, Talim B, Erdem S, Akcören Z, Tan E, Caglar M, Richard I, Nigro V, *et al*: Calpain-3 mutations in Turkey. Eur J Pediatr 165: 293-298, 2006.
54. de Paula F, Vainzof M, Passos-Bueno MR, de Cássia M Pavanello R, Matioli SR, V B Anderson L, Nigro V and Zatz M: Clinical variability in calpainopathy: What makes the difference? Eur J Hum Genet 10: 825-832, 2002.
55. Fanin M, Nascimbeni AC, Fulizio L and Angelini C: The frequency of limb girdle muscular dystrophy 2A in northeastern Italy. Neuromuscul Disord 15: 218-224, 2005.
56. Fanin M, Nascimbeni AC, Tasca E and Angelini C: How to tackle the diagnosis of limb-girdle muscular dystrophy 2A. Eur J Hum Genet 17: 598-603, 2009.
57. Dorobek M, Ryniewicz B, Kabzińska D, Fidziańska A, Styczyńska M and Hausmanowa-Petrusewicz I: The Frequency of c.550delA mutation of the CANP3 gene in the Polish LGMD2A population. Genet Test Mol Biomarkers 19: 637-640, 2015.
58. Piluso G, Politano L, Aurino S, Fanin M, Ricci E, Ventriglia VM, Belsito A, Totaro A, Saccone V, Topaloglu H, *et al*: Extensive scanning of the calpain-3 gene broadens the spectrum of LGMD2A phenotypes. J Med Genet 42: 686-693, 2005.
59. Pogoda TV, Krakhmaleva IN, Lipatova NA, Shakhovskaya NI, Shishkin SS and Limborska SA: High incidence of 550delA mutation of CAPN3 in LGMD2 patients from Russia. Hum Mutat 15: 295, 2000.
60. Milic A and Canki-Klain N: Calpainopathy (LGMD2A) in Croatia: Molecular and haplotype analysis. Croat Med J 46: 657-663, 2005.
61. Duguez S, Bartoli M and Richard I: Calpain 3: A key regulator of the sarcomere? FEBS J 273: 3427-3436, 2006.
62. Foley AR, Donkervoort S and Bönnemann CG: Next-generation sequencing still needs our generation's clinicians. Neurol Genet 1: e13, 2015.
63. Şahin İO, Özkul Y and Dündar M: Current and future therapeutic strategies for limb girdle muscular dystrophy type R1: Clinical and experimental approaches. Pathophysiology 28: 238-249, 2021.
64. Li C and Samulski RJ: Engineering adeno-associated virus vectors for gene therapy. Nat Rev Genet 21: 255-272, 2020.

Copyright © 2024 Mao et al. This work is licensed under a Creative Commons Attribution-NonCommercial-NoDerivatives 4.0 International (CC BY-NC-ND 4.0) License.